Evaluation of Angle of Arrival in Indoor Environments with Bluetooth 5.1 Direction Finding

Michele Girolami, Paolo Barsocchi, Francesco Furfari, Davide La Rosa, Fabio Mavilia
Italian National Council of Research, ISTI-CNR, Pisa, Italy
Email: {name.surname}@isti.cnr.it

Abstract—The Bluetooth 5.1. Direction Finding (DF) specification opens to the possibility of estimating the angle between an emitting and a receiving device. Such angle is generally measured estimating the Angle of Arrival (AoA) or the Angle of Departure (AoD). In particular, knowledge about AoA between a set of anchor nodes and a moving target could be used to localize the target, with greater accuracy with respect to traditional approaches based on the Received Signal Strength of the received messages. In this work, we rigorously evaluate the performance of a commercial kit implementing the DF specification, with the purpose of understanding how the AoA measure varies with respect to the angles' ground truth. We describe two real-world experimental scenarios and we compute the errors between the estimated and actual angles. We also discuss three key aspects for the purpose of adopting BT 5.1 in indoor localization applications.

Keywords-Bluetooth 5.1, Direction Finding, Indoor localization, Proximity

I. Introduction

Recently, the Bluetooth Special Interest Group (Bluetooth SIG) has presented a new feature called Direction Finding (DF) in extension to the Bluetooth Core Specification 5.1. The DF specification is targeted to indoor positioning, asset tracking and directional discovery [1]. The standard has supplemented two signal processing techniques enabling the receiving device to estimate the direction of the transmitting signal, namely the Angle-of-Arrival (AoA) and Angle-of-Departure (AoD). Concerning the AoA, the receiver is equipped with an antenna array and a micro-controller to compute the direction of the received signal by measuring the phase delay at multiple antennas. On the other hand, the computation of the AoD requires the transmitter to be equipped with an antenna array that periodically sends a signal, enabling the receivers to detect the direction of the source [2].

Despite the potentiality of such technology, few experimental studies have been conducted to evaluate the accuracy of Direction Finding. In this work, we study the performance of a commercial kit, namely the XPLR-AOA produced by ublox in a realistic setting. We test the estimation of the AoA with two receiving devices (the anchor nodes) positioned at different heights from the ground and at different inclinations with respect to the load-bearing wall. We position the emitting device (the tag node) on 28 different locations, so that to test the AoA evaluation with a variety of angles both on the azimuth and elevation planes. The goal of this work is

twofold. On the one hand, we rigorously set up a performance assessment of a DF-ready chipset in order to understand the potentiality of AoA estimation in indoor environments. On the other hand, we derive some considerations about the deployment of the anchor nodes for the purpose of evaluating an indoor localization system based on the AoA and Received Signal Strength (RSS) [3], [4] features. We show in this work how the estimation error of the AoA varies at different angles, and we report some discussions with 3 take-away messages: coverage area of the anchor nodes, optimal positioning and the low variation of the estimated AoA. Our experimental results show that the AoA estimation considerably differs for the azimuth and elevation planes. In particular, we identify a triangular region where the AoA fits with the ground truth angles, while some peripheral areas where the AoA estimation quickly drops.

In Section II we survey existing experimental settings based on BT 5.1, Section III summarizes the background of AoA estimation. Finally, Section IV details our experimental settings and Section V reports the description of our data collection campaign with the obtained results, as well as a discussion on the applicability of BT 5.1 for the purpose of an indoor localization system.

II. Related Work

The current literature reports several experimental studies estimating the accuracy of Bluetooth 5.1 Direction Finding's functionality. The majority of these studies have been conducted by using hardware emulation, hence not fully reproducing real-world conditions obtainable with commercial off-the-shelf (COTS) Bluetooth devices.

In [5], authors evaluate the position of a Bluetooth Low Energy (BLE) tags advertising BLE beacons using Software Defined Radio (SDR) obtaining a limited margin of error, in the range of $-60°$ to $60°$. Also in [6], SDR has been used to emulate the specification of BLE packets with Constant Tone Extension (CTE, as described in Section III). The proposed approach has obtained an accuracy of the AoA measurements of $5°$ for a range of $15°$ to $90°$, with standard deviations from the true angle between $0.2°$ and $2°$. Moreover, the estimated positioning errors are below 0.85m for 95% of the true positions tested. The approach proposed in [7] relies on mobile receivers equipped with antenna arrays and a fixed infrastructure composed of battery-powered beacons. The solution has been tested implementing a simulator and using a dataset

of AoA measurements. The position estimation accuracy is less than 1 meter, employing 1 beacon per $15m^2$ at $2\ Hz$ of transmission rate. One of the few works based on COTS devices is described in [8]. Authors perform an experimental study in indoor and outdoor environments relying on the Texas Instruments CC26X2R transceiver and the BOOSTXL-AOA[1] antenna array board. The authors demonstrate a greater angular and positioning error in an indoor environment due to some obstructions in the room, causing the multi-path effect and degrading the positioning performance. Similar results have been reached in [9]. Authors test the proposed localization system in indoor and outdoor maritime scenarios, obtaining an AoA accuracy of 87%. Finally, in [10] authors perform a positioning experimental study between BLE and UWB technologies. They demonstrate that BLE is more affected by multi-path interference in indoor environments, as well as the presence of WiFi signals.

III. BLUETOOTH 5.1 DIRECTION FINDING

The BLE wireless protocol is commonly adopted for inexpensive, low-power consumption and low-data rate small-size networks. The BLE tags advertise beacons, small packets used to broadcast few bit of information to devices in proximity. A device equipped with an antenna array can determine the AoA of signals from a transmitter using RF radiogoniometry techniques [2]. AoA is computed by measuring the phase difference γ between signals received at each pair of neighboring antennas, knowing both the wavelength λ of the signal and the distance d between the antennas. The angle of arrival θ can be calculated by the formula: $\theta = \arccos(\frac{\lambda\gamma}{2\pi d})$.

Preamble (1 or 2 octets)	Access-Address (4 octets)	PDU (2-258 octets)	CRC (3 octets)	Constant Tone Extention (16-160 μs)

Fig. 1: Bluetooth packet format supporting Direction Finding capability.

In order to support the direction finding capability, BLE packets embed an additional field called Constant Tone Extension (CTE), that follows the CRC code, as showed in Fig. 1. The CTE consists of a constantly modulated sequence of unwhitened 1-valued bits, with variable length between 16–160 μs, to guarantee a constant frequency for this part of the signal. The receiver, throughout the CTE part of the BLE packet, is able to collect In-Phase and Quadrature (IQ) samples of the signal for every array's antenna. The IQ samples are used to estimate the information about the received signal, such as wavelength and frequency, and to calculate the angle-of-arrival.

IV. THE EXPERIMENTAL SETTINGS

We now detail the settings of our experimental data collection campaign. We first describe the adopted hardware and then we detail the environment used for our experiments.
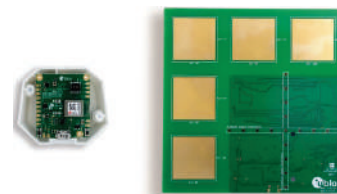

Fig. 2: The XPLR-AOA explorer kit: the tag and the anchor.

A. The Hardware Kit

We use the XPLR-AOA explorer kit by ublox for our data collection campaign. Anchor's boards are 11.5x11.5 cm and they are equipped with an array of 5 square-shaped C211 antennas. Moreover, the board is equipped with the NINA-B411[2] BLE module and an USB port for I/O operations. Anchors support AT serial commands through which it is possible to configure the anchor's output and other settings.

The C209 tag embeds the NINA-B406[3] BLE module and it is encapsulated in a plastic box for an easy deployment. Tags use 3 Bluetooth channels (37, 38 and 39) for advertising Eddystone[4]-based beacons. Tags allow to set the advertisement rate and the power of transmission. The advertisement rate determines the frequency of the beacon's advertisement, and it can vary in the range: 1, 10 or 50 Hz. The transmission power can be selected within a set of 15 pre-configured values, ranging from $-40\ dBm$ to $8\ dBm$. Anchors and tags are shown in Fig. 2.

Anchors can be provisioned with a specific firmware delivered by ublox which estimates, for each received beacon, the following metrics: (i) the AoA between the tag's position and the azimuth plane (xy plane reported in Fig. 3) and the corresponding Received Signal Strength (RSS), (ii) the AoA between the tag's position and the elevation plane (zy plane reported in Fig. 3) with the corresponding RSS value, (iii) the advertisement channel and (iv) a relative timestamp.

B. The Experimental Layout

Data computed by the anchor nodes are collected in a wide room located in our research institute, CNR-ISTI Pisa, Italy. The room is 110.4 m^2 (13.8x8.0 m) with an height of 3.1 m, it is empty and the floor is composed of 60x60 cm regular tiles. We deploy 2 anchors, namely B and A, positioned on the wall at 2 different heights, as shown in Fig. 3. In particular, B lies parallel with respect to the wall at 110 cm above the ground, while A is tilted $\alpha = 32°$ with respect to the wall and 266 cm above the ground, hence pointing to the center of the room.

The tag is positioned according to a regular grid as reported in Fig. 3. More specifically, we identified 28 locations equally spaced from each other by 180 cm along both the x and y axes. The identified locations allow us to test a variety

---

[1]https://www.ti.com/tool/BOOSTXL-AOA
[2]https://www.u-blox.com/en/docs/UBX-20035327
[3]https://www.u-blox.com/en/docs/UBX-19049405
[4]https://github.com/google/eddystone

of angles obtained between the tag and the anchor on the azimuth and elevation planes. In particular, the range of the experimented angles on the azimuth varies from -77° (location `540,120`) to 77° (location `-540,120`), while the range for the elevation varies from -20° (location `0,120`), to 19° (location `0,660`).

We deploy the tag according to 2 settings:

- Setting 1: tag held by a tripod at 110 cm above the ground, in front of the anchors;
- Setting 2: tag held with a badge holder by a person, the tag is at 110 cm above the ground, in front of the anchors. This setting allows us to test the hardware kit for the purpose of localizing a moving target holding the tag device.

For each of the 2 settings, we position the tag in the 28 locations and we collect the data generated by the 2 anchors for 2 minutes. As a result, we logged about 2 hours of aggregated data from each of the anchors.
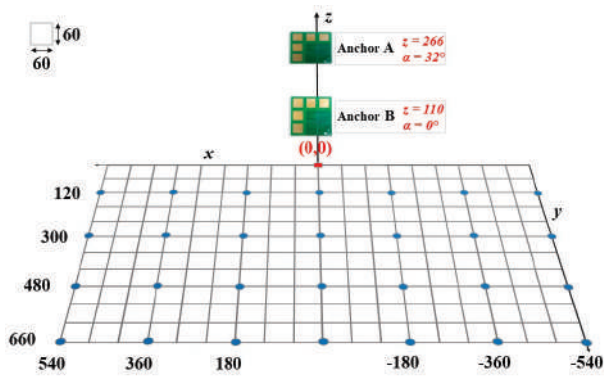
Fig. 3: The experimental area, the blue dots represent the locations of the tag, while the anchors are positioned at 2 different heights and inclinations from the ground.

V. EXPERIMENTAL RESULTS AND DISCUSSION

We now detail our analysis concerning the errors between the real and estimated angles. Section V-A describes the process we implement to compute the ground truth, namely the real angles between the tag and the anchor, while Section V-B reports our results and Section V-C discussion.

A. Computing the Ground Truth of the Angles

As described in Section IV-B, the tag is positioned in 28 different locations, as reported with the grid in Fig. 3. We now detail how we compute the existing angles between the tag and the anchors, both for the azimuth and elevation planes. The obtained angles represent our ground truth (GT) that we compare with the estimated AoA in Section V-B.

Azimuth plane: the angle ϕ on the azimuth plane between the tag and the anchor A is shown in Fig. 4. The red circle represents the location of the tag (x, y), from which we can obtain $\phi = \arctan(x/y)$. The same process can be followed with anchor B.
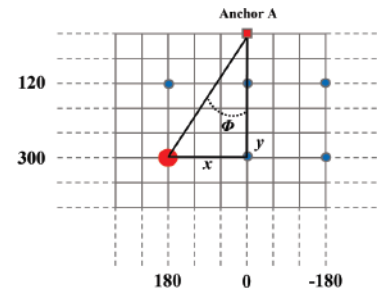
Fig. 4: Angle between the tag and the anchor on the azimuth plane.

Elevation plane: differently from the azimuth plane, the elevation angle does not vary between the tag and anchor B, as anchor B and the tag lay at the same altitude with respect to the floor (110 cm). On the contrary, we measure the angle δ between the tag and anchor A, as shown in Fig. 5. The figure shows the side view on the plane of the y, z axes with $x = 0$. Given the height of the tripod $z_T = 110$ cm, it is possible to determine the elevation angle $\delta(x, y)$ that anchor A measures, by observing the tripod placed in a fixed position of the plane. A first calculation method is based on the application of Carnot's theorem:

$$\overline{\text{TP}}^2 = \overline{\text{AT}}^2 + \overline{\text{AP}}^2 - 2 \cdot \overline{\text{AT}} \cdot \overline{\text{AP}} \cdot \cos(\delta)$$

However, from the Carnot's theorem it is not possible to calculate the negative elevation that is measured when the tripod is below the inclined plane. A different approach is computing $\delta = \beta - \theta$. In particular, as reported in Fig. 5, we obtain: $\beta = \arccos(\overline{\text{AC}}/\overline{\text{AP}})$ and $\theta = \arctan(\overline{\text{CT}}/\overline{\text{AC}})$.
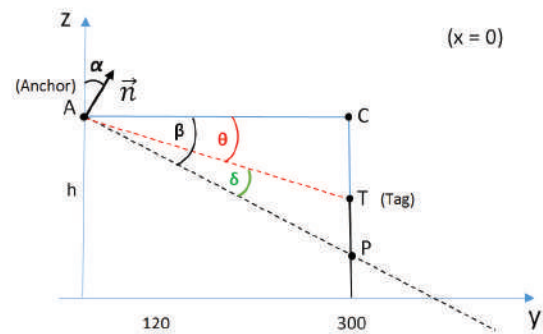
Fig. 5: Angle δ between the tag T and anchor A on the elevation plane.

Proceeding analytically, the equation of the anchor's inclined plane can be written using the vector normal to the plane $\overrightarrow{n} = (0, \sin(\alpha), \cos(\alpha))$ with α corresponding to the anchor's inclination. By imposing the constraint that the plane crosses the point $A = (0, 0, h)$, we obtain the following plane's equation $z = h - \tan(\alpha) \cdot y$. By intersecting the plane with the sphere centered in A, we can derive the distance $r(x, y)$ from anchor A of a point (x, y) projected on the inclined plane (i.e. point P in Fig. 5) : $x^2 + y^2 + (z - h)^2 = r^2$. Setting
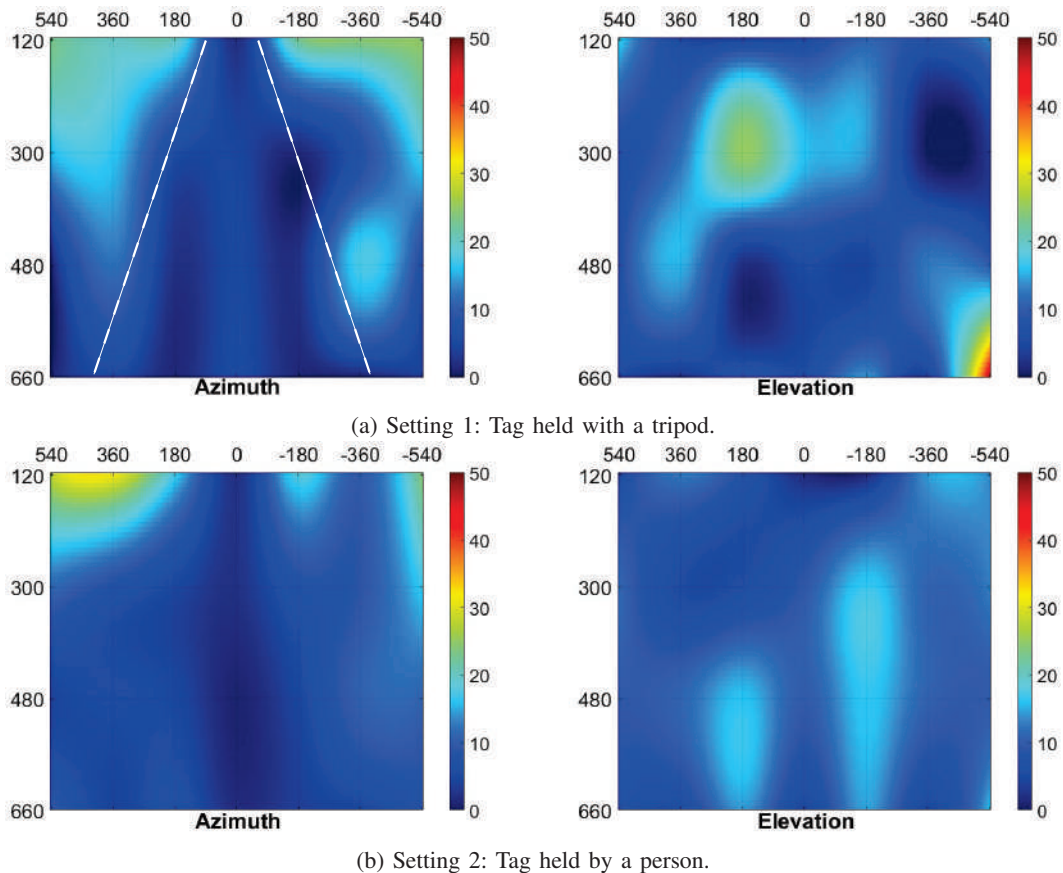
(a) Setting 1: Tag held with a tripod.

(b) Setting 2: Tag held by a person.

Fig. 6: Scenario 1: variation of the Mean Absolute Error (MAE) with anchor A ($z = 266\ cm, \alpha = 32°$), Settings 1 and 2.

$D = \sqrt{x^2 + y^2}$, the euclidean distance on the x,y plane (segment $\overline{AC}$, in Fig. 5), with the appropriate substitutions for the angle $\beta(x, y, \alpha)$ we have:

$$\beta = \arccos\left(\frac{D}{\sqrt{x^2 + y^2 \cdot (1 + tg^2(\alpha))}}\right)$$

and

$$\theta = \arctan\left(\frac{h - z_T}{D}\right)$$

which allows us to determine the angle δ between the tag and anchor A.

B. Evaluation of the AoA

In this section, we analyze the errors resulting from the comparison between the GT's AoA and the AoA estimated by anchors A and B on the azimuth and elevation planes, with respect to the tag positioned according to Setting 1 and 2 (see Section IV-B). With Setting 1, the tag is positioned on a tripod while with Setting 2, the tag is held around the neck by a person. In summary, we measure the performance of XPLR-AOA kit on the following 2 Scenarios:

- Scenario 1: anchor A applied to Settings 1,2 as shown in Fig. 6.
- Scenario 2: anchor B applied to Settings 1,2 as shown in Fig. 7;

The heat maps report a graphical representation of the mean absolute error (MAE) computed between the GT'angles (ϕ_i and δ_i) and the estimated ones ($\hat{\phi}_i$ and $\hat{\delta}_i$). As for example, concerning the azimuth plane and the elevation planes, the two following metrics are used:

$$MAE_\phi = \frac{\sum_{i=1}^n |\phi_i - \hat{\phi}_i|}{n}; MAE_\delta = \frac{\sum_{i=1}^n |\delta_i - \hat{\delta}_i|}{n} \quad (1)$$

We report in Table I the standard deviation, MAE and RMSE (Root Mean Square Error) of the AoA in both scenarios.

Concerning the azimuth plane, we observe a region with low values of the MAE. The region fits with a triangular shape centered in (0,0) and expanding towards the center of the room. This trend is particularly evident for Scenario 1 and Setting 1,2 where it is possible to observe a cone starting from the location of anchor A (white cone in Fig. 6). Differently, the MAE generally increases in peripheral regions, such as locations (−360,120), (−540,120) and locations (360,120), (540,120) reported in Fig. 6. Concerning Scenario 2, the MAE is even lower in such peripheral regions, as visible in locations (360,120) and (540,300) of Fig. 7. Such variations are caused by the different position of the anchor. Indeed, with Scenario 1 the anchor points to the center of the room ($z = 266\ cm$ and $\alpha = 32°$) enabling the anchor to well estimate the tag's AoA. Differently, in the Scenario 2
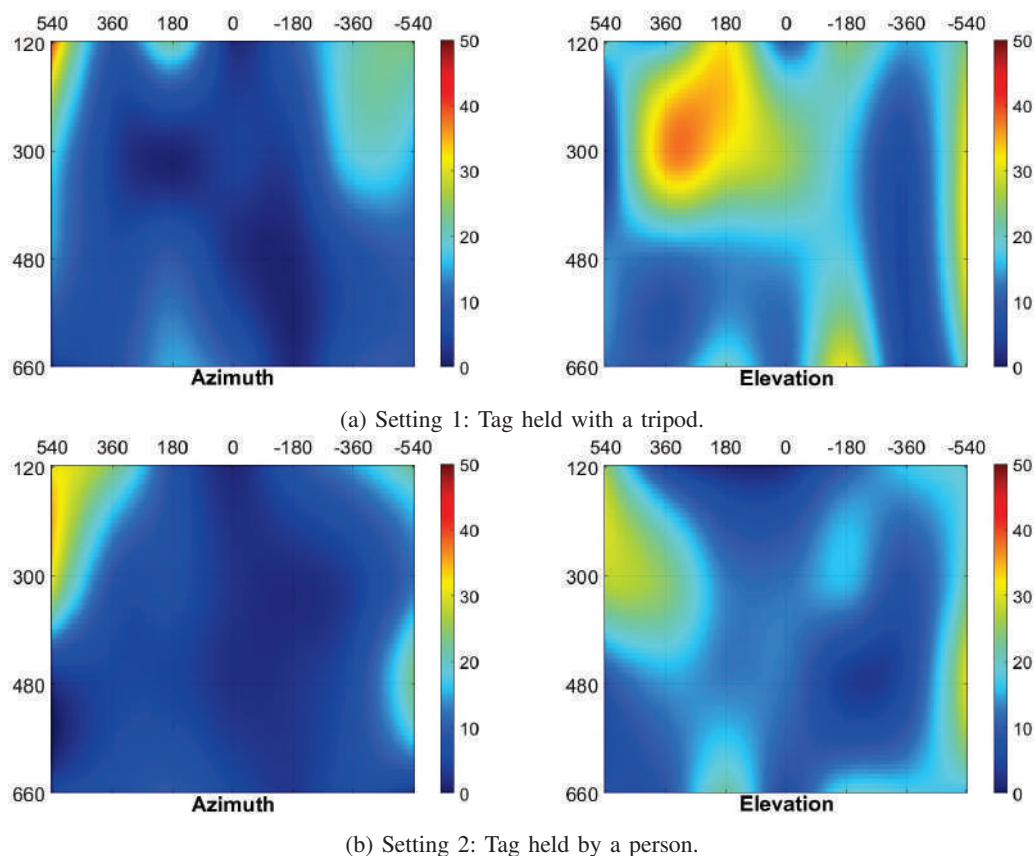
(a) Setting 1: Tag held with a tripod.

(b) Setting 2: Tag held by a person.

Fig. 7: Scenario 2: variation of the Mean Absolute Error (MAE) with anchor B ($z = 110\ cm, \alpha = 0°$), Settings 1 and 2.

the anchor is parallel to the wall, positioned at $110\ cm$ above the ground and with a reduced visibility of peripheral areas.

We also observe some remarkable differences on the estimation of the AoA when the tag is positioned on the tripod or held by a person. In Scenario 2, we measure a slight decrease of the MAE, varying from 10.66° for Setting 1 to 9.28° for Setting 2.

For what concerns the elevation plane, we observe a general reduction of the performance, as evident from the heat maps. More specifically, for Setting 1 and for both scenarios, we detect the existence of a central region centered in (180, 399) with high values of the MAE.

Finally, for what concerns the standard deviation of the estimated AoA, our measurements reveal that in both of the scenarios the AoA varies slightly over the 2 minutes of data collection. In particular, the standard deviation is bound in the range 1.22° for Scenario 2, Setting 1 to 5.43° for Scenario 1, Setting 2. However, the higher standard deviations were measured when the beacon was held with a badge holder by a person.

C. Discussion

The data collection campaign described in this work allows us to derive some considerations about the adoption of Bluetooth 5.1 devices in indoor environments. More specifically, we are interested in adopting such technology for the purpose

TABLE I: Evaluation metrics of AoA on azimuth and elevation planes, applied to every Scenario and Setting.

			STD DEV	MAE	RMSE
Anchor A (tilted)	Azimuth ϕ	Tripod	1.51	9.64	12.95
		Person	3.87	9.73	13.34
	Elevation δ	Tripod	1.27	10.30	14.05
		Person	5.43	10.09	12.29
Anchor B (parallel)	Azimuth ϕ	Tripod	1.22	10.66	13.76
		Person	3.37	9.28	16.44
	Elevation δ	Tripod	1.90	18.29	20.69
		Person	5.58	13.93	17.65

of indoor localization and proximity detection as also studied in [11].

Coverage Areas: we can identify a bounded region, where the estimation of the AoA on the azimuth plane matches with the GT, as shown with the white triangular shape in Fig. 6. Identifying the exact width of such a shape is not possible, but as a general trend, the estimation of the AoA decreases in the peripheral area aligned with the location of the anchor. Indeed, such locations correspond to the maximum angles between the tag and the anchors, ie. -77° (location 540, 120) and 77° (location −540, 120), leading to high AoA inaccuracies. Therefore, the first consideration is that each anchor node has a limited coverage area. Fig. 8a shows a 3D representation
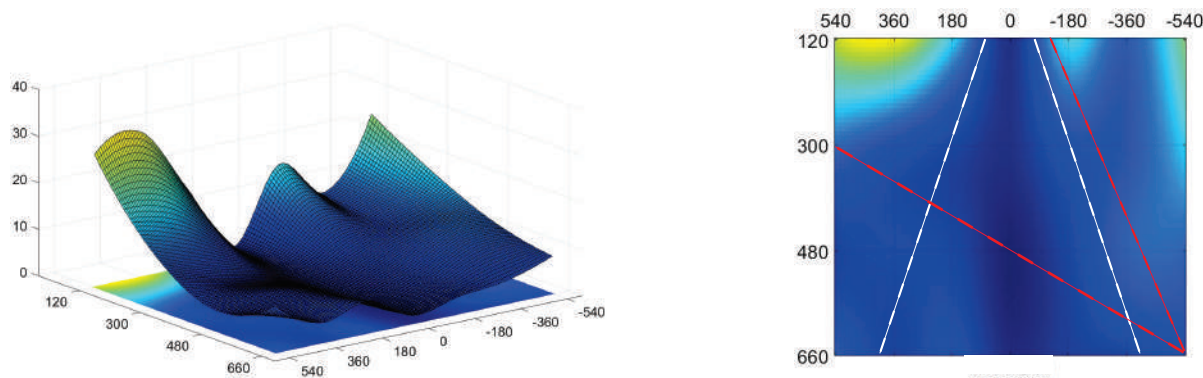
(a) 3D representation of the MAE in Scenario 1.

(b) A possible deployment of two opposite anchor nodes.

Fig. 8: Graphical representation of the MAE variation and anchor node deployment.

of the MAE in which is evident the tendency to increase in the peripheral regions. The size of the room could also influence the AoA accuracy due to signal reflections on the walls, indeed in larger rooms we expect an improvement of the AoA estimation corresponding to a widening of the triangular shape shown in Fig. 6.

Optimal Positioning: the existence of a preferential region with low values of the MAE, lead us to consider the possibility of deploying multiple anchors, so that to intersect the triangular regions and to compensate the errors. More specifically, the deployment of 2 opposite anchors would lead to a compensation of the low-performing areas, as anchor 1 would cover the inaccuracies of anchor 2 and vice-versa, as shown by the two triangular regions in Fig. 8b. The deployment of a second anchor (red dashed line), covers the bottom right region with high MAE values.

Low AoA Variations: our measurements show that the estimation of the AoA is stable along the time. More specifically, the anchors estimate the AoA with few variations in stable conditions. As reported in Table I, the standard deviation varies in a very limited range.

VI. CONCLUSIONS

In this work we analyze the performance of the XPLR-AOA kit produced by ublox based on Bluetooth 5.1 Direction Finding specification. The kit allows to estimate the Angle of Arrival between tag and anchor node both on the azimuth and elevation planes. We set up an experimental environment in which we compare the AoA estimated by the kit with respect to the ground truth of the AoAs. To this purpose, we define two experimental scenarios, in which the anchor is positioned both at the same height of the tag or placed at $266\ cm$ from the floor and tilted toward the center of the room. We also position the tag on a fixed tripod and around the neck of a person. We identify 28 locations for the tag, ranging from $-77°$ to $77°$ on the azimuth plane, and from $20°$ to $-19°$ on the elevation plane. Our experiments show the variation of the mean absolute error, root mean square error and the standard deviation of the estimated AoA. From our experiments, we identify a typical triangular region where the estimation of

the AoA is generally correct with respect to the ground truth. Differently, we also identify some critical areas where the AoA's estimation is not correct. Our experimental setting represents a preliminary study to evaluate the performance of a fully-compliant kit implementing the Bluetooth 5.1 features. Further lines of investigation include the adoption of this kit to test some indoor localization algorithms based on AoA on different planes and with a moving target. We also plan to combine the use of RSS estimated by the anchors with the AoA computation.

REFERENCES

[1] M. Woolley, "Bluetooth direction finding," *A technical Overview*, 2019.

[2] G. Pau, F. Arena, Y. E. Gebremariam, and I. You, "Bluetooth 5.1: An analysis of direction finding capability for high-precision location services," *Sensors*, vol. 21, no. 11, p. 3589, 2021.

[3] M. Girolami, F. Mavilia, and F. Delmastro, "Sensing social interactions through ble beacons and commercial mobile devices," *Pervasive and Mobile Computing*, vol. 67, p. 101198, 2020. [Online]. Available: https://www.sciencedirect.com/science/article/pii/S1574119220300675

[4] P. Cassarà, F. Potortì, P. Barsocchi, and M. Girolami, "Choosing an rss device-free localization algorithm for ambient assisted living," in *2015 International Conference on Indoor Positioning and Indoor Navigation (IPIN)*, 2015, pp. 1–8.

[5] F. A. Toasa, L. Tello-Oquendo, C. R. Peafiel-Ojeda, and G. Cuzco, "Experimental demonstration for indoor localization based on aoa of bluetooth 5.1 using software defined radio," in *2021 IEEE 18th Annual Consumer Communications & Networking Conference (CCNC)*. IEEE, 2021, pp. 1–4.

[6] M. Cominelli, P. Patras, and F. Gringoli, "Dead on arrival: An empirical study of the bluetooth 5.1 positioning system," in *Proceedings of the 13th international workshop on wireless network testbeds, experimental evaluation & characterization*, 2019, pp. 13–20.

[7] N. Paulino, L. M. Pessoa, A. Branquinho, and E. Gonçalves, "Evaluating a novel bluetooth 5.1 aoa approach for low-cost indoor vehicle tracking via simulation," in *2021 Joint European Conference on Networks and Communications & 6G Summit*. IEEE, 2021, pp. 259–264.

[8] P. Sambu and M. Won, "An experimental study on direction finding of bluetooth 5.1: Indoor vs outdoor," *arXiv:2103.04121*, 2021.

[9] A. Mohanna, F. Cardinali, and D. Anghinolfi, "Maritime localization system based on iot," in *2021 28th IEEE International Conference on Electronics, Circuits, and Systems (ICECS)*. IEEE, pp. 1–5.

[10] L. Botler, M. Spörk, K. Diwold, and K. Römer, "Direction finding with uwb and ble: A comparative study," in *2020 IEEE 17th International Conference on Mobile Ad Hoc and Sensor Systems (MASS)*. IEEE, 2020, pp. 44–52.

[11] B. Wang, Y. Wang, X. Qiu, and Y. Shen, "Ble localization with polarization sensitive array," *IEEE Wireless Communications Letters*, vol. 10, no. 5, pp. 1014–1017, 2021.